Mechanisms of orexin-induced depolarizations in rat dorsal motor nucleus of vagus neurones *in vitro*

Ling-Ling Hwang, Chiung-Tong Chen and Nae J. Dun

Department of Pharmacology, James H. Quillen College of Medicine, East Tennessee State University, PO Box 70577, Johnson City, TN 37614, USA

(Resubmitted 14 May 2001; accepted after revision 16 August 2001)

1. Whole-cell patch-clamp recordings were made from neurones of the dorsal motor nucleus of the vagus (DMNV), including Fluoro-gold-labelled parasympathetic preganglionic neurones (PPNs), in slices of the rat medulla. In the latter case, rats had received an I.P. injection of Fluoro-gold solution (10 μg) 2–3 days earlier.

2. Superfusion of orexin A or B (10–300 nM) caused a slow depolarization in approximately 30 % of the DMNV neurones, including PPNs. Orexin-induced depolarizations, which persisted in TTX (0.5 μM)-containing Krebs solution, were reduced by 70 % in a low-Na^+ (26 mM) Krebs solution, indicating the involvement of Na^+ ions. A significant change in orexin-induced depolarizations was not obtained in either a high-K^+ (7 mM) or Cd^{2+} (100 μM) Krebs solution.

3. Inclusion of the hydrolysis-resistant guanine nucleotide GDP-β-S in the patch solution significantly reduced the orexin A- or B-induced depolarizations.

4. Under whole-cell voltage-clamp conditions, the orexin-induced inward current declined with hyperpolarization, but did not reverse polarity in the potential range between −120 and 0 mV. In low-Na^+ solution, the orexin-induced current was reduced, and the I–V curve reversed polarity at about −105 mV; the response was further reduced and the reversal potential shifted to −90 mV in a low-Na^+, high-K^+ Krebs solution.

5. It is concluded that the peptides orexin A and B, acting on orexin receptors, which are GTP-binding-protein coupled, are excitatory to DMNV neurones. In addition, more than one conductance, which may include a non-selective cation conductance and a K^+ conductance, appears to be involved in the orexin-induced depolarization.

Orexin A and B, also known as hypocretin 1 and 2, respectively, are two recently isolated hypothalamic peptides (de Lecea *et al.* 1998; Sakurai *et al.* 1998). Orexin A is a 33 amino acid peptide and orexin B a 28 amino acid peptide; 46 % sequence homology exists between the two (Sakurai *et al.* 1998). Initial studies suggest that these peptides may be involved in food intake and positive energy metabolism in the rat (Sakurai *et al.* 1998). For example, prepro-orexin mRNA and orexin A immunoreactivity have been reported to occur in neurones of the rat lateral and posterior hypothalamus (de Lecea *et al.* 1998; Sakurai *et al.* 1998; Chen *et al.* 1999), which have long been suspected to play a central role in feeding behaviour (Bernardis & Bellinger, 1993, 1996). Furthermore, prepro-orexin gene expression is up-regulated in fasting rats (Sakurai *et al.* 1998) and decreased in genetically obese mice (Yamamoto *et al.* 1999). Functionally, the intracerebroventricular injection of orexin A or B promotes food consumption in rats (Sakurai *et al.* 1998). The site(s) and mechanism whereby orexin may induce food intake are not known.

The potential importance of orexins in food consumption notwithstanding, more recent studies suggest that orexins mediate the cephalic phase of gastric secretion (Takahashi *et al.* 1999). For example, orexin A-immunoreactive fibres are distributed throughout the rat brainstem including the nucleus of the solitary tract and dorsal motor nucleus of the vagus (DMNV; Date *et al.* 1998; Peyron *et al.* 1998; Harrison *et al.* 1999). When injected intracisternally, orexin A but not orexin B increases gastric acid secretion in rats, and this effect is blocked by vagotomy or by atropine (Takahashi *et al.* 1999). DMNV neurones are the major source of parasympathetic innervation to the subdiaphragmatic visceral organs, which control gastro-intestinal and pancreatic secretion as well as stomach and small intestinal motility (Loewy & Spyer, 1990). Viewed in this context, DMNV neurones may be an important site upon which orexins exert their influence in the gastro-intestinal tract. The present study was undertaken to evaluate, at a cellular level, the actions of orexins on DMNV neurones including the parasympathetic preganglionic neurones (PPNs).

METHODS

Medullary slices and electrophysiological procedures

Sprague-Dawley rats, 15–20 days old, of either sex (Harlan, Indianapolis, IN, USA), were used in this study. For the purpose of labelling the PPNs (Leong & Ling, 1990; Merchenthaler, 1991), the rats received an I.P. injection (10 μg) of the retrograde fluorescent dye Fluoro-gold 2–3 days prior to experimentation. Experimental protocols were reviewed and approved by the University Animal Care and Use Committee.

Rats were anaesthetized with urethane (1.2 g kg^{-1}, I.P.) and the brainstem was rapidly removed and placed in chilled, oxygenated Krebs solution, as described previously (Hwang & Dun, 1998, 1999). Three 400 μm-thick coronal slices, starting from about 600 μm caudal to the obex and moving rostrally, were obtained using a vibratome. The Krebs solution had the following composition (mM): 127 NaCl, 1.9 KCl, 1.2 KH_2PO_4, 2.4 $CaCl_2$, 1.3 $MgCl_2$, 26 $NaHCO_3$ and 10 glucose, and was saturated with 95% O_2 and 5% CO_2. The low-Na^+ (26 mM) Krebs solution was prepared by replacing NaCl with Tris-buffer and the pH was titrated to 7.4 with HCl. In preparing the high-K^+ (7 mM) Krebs solution, KCl was increased and NaCl decreased accordingly. In the experiment where Cd^{2+} was applied, KH_2PO_4 was replaced by an equimolar amount of KCl. All experiments were conducted at room temperature (20 ± 1 °C).

The whole-cell patch-clamp recording technique used was similar to that described by Hwang & Dun (1998, 1999). Patch electrodes filled with a solution containing (mM): 125 potassium gluconate, 5 KCl, 1 $MgCl_2$, 0.4 $CaCl_2$, 5 ATP, 0.3 GTP, 2 EGTA, 10 Hepes and 10 sucrose, and in some cases, 0.2% lucifer yellow, had a resistance of 2–5 MΩ; the pH of the solution was adjusted to 7.2 with KOH.

Signals were recorded using an Axopatch-1C (Axon Instruments), low-pass filtered at 2 kHz and acquired using a personal computer and pCLAMP software (version 7.0, Axon Instruments) for later analysis. Signals were also recorded with a two-channel Gould chart recorder RS3200. Membrane potentials reported in the text were corrected for liquid-junction potentials. The access resistance was less than 25 MΩ.

In the voltage-clamp experiments, the steady-state current–voltage (I–V) relationship was obtained by applying a series of 1 s voltage command steps every 5 s from a holding potential of −60 mV to different potentials (−120 to 0 mV) with 10 mV increments before and during the application of orexin in TTX-containing (0.5 μM) Krebs solution. The current value was measured at the end of each step. Currents elicited by such voltage commands in control media were subtracted from their counterparts in the presence of orexin to yield steady-state I–V curves of orexin-induced currents.

Immunohistochemical procedures

For the purpose of labelling the PPNs, rats received an I.P. injection of Fluoro-gold (10 μg) 2–3 days earlier. To identify the recorded neurone, the patch electrodes were filled with a solution containing the fluorescent dye lucifer yellow (0.2%), which was allowed to diffuse into the recorded neurone. At the end of recording, the slice was placed in 4% paraformaldehyde in 0.1 M phosphate-buffered saline (PBS) overnight, and then transferred to a solution of 30% sucrose in PBS until further processing. The slice was sectioned at 50 μm using a cryostat. Sections were examined with the aid of a microscope and the section containing the lucifer yellow-labelled neurone was selected and processed further for Fluoro-gold immunoreactivity. The section was first blocked with 10% normal goat serum and then incubated with rabbit polyclonal Fluoro-gold antiserum (1:3000) for 24 h at room temperature, followed by 24 h in a cold room with gentle agitation. After several washes with PBS, the section was incubated with biotinylated goat anti-rabbit IgG (1:50 dilution) for 3 h followed by Avidin Texas Red (1:50 dilution) for 4 h. Finally, the section was washed for 30 min with PBS, mounted in Citifluor (Ted Pella) and coverslips applied.

The chemicals and reagents used in these experiments were obtained from the following suppliers: orexin A and B from Phoenix Pharmaceuticals (Belmont, CA, USA); Fluoro-gold from Fluochrome (Denver, CO, USA); TTX from Research Biochemicals (Natick, MA, USA); lucifer yellow, (−)-bicuculline methiodide, guanosine 5′-O-(2-thiophosphate) trilithium salt (GDP-β-S), and all other chemical reagents from Sigma Chemicals (St Louis, MO, USA). The rabbit polyclonal Fluoro-gold antiserum was from Chemicon International (Temecula, CA, USA) and all other reagents for immunohistochemistry were from Vector Laboratories (Burlingame, CA, USA).

Data are expressed as means ± S.E.M. and were analysed statistically using Student's t test; $P < 0.05$ was considered statistically significant.

RESULTS

Membrane properties of DMNV neurones

Stable recordings were made from 151 DMNV neurones in brainstem slices from 87 rats. The mean resting membrane potential, input resistance and amplitude of action potentials was −55 ± 1 mV ($n = 104$), 696 ± 37 MΩ ($n = 104$) and 67 ± 1 mV ($n = 151$), respectively. Forty-seven neurones exhibited a relatively high discharge frequency; consequently, the resting membrane potential and input resistance of these neurones were not measured.

Effects of orexin A and orexin B on DMNV neurones

Orexin A or orexin B (10–300 nM) applied by perfusion for a period of 2–4 min excited approximately 30% (36 of 120) and 32% (20 of 63) of the DMNV neurones, as manifested by a membrane depolarization and/or increase of neuronal discharges (Fig. 1*A* and *B*). Membrane potentials nearly recovered to the control level 20–40 min after removing the peptide from the bath. For a given concentration, the depolarization varied considerably among the different cells tested. Orexin A at concentrations of 10 and 100 nM caused a mean depolarization of 1.9 ± 1.1 mV ($n = 4$) and 9.0 ± 1.2 mV ($n = 26$), respectively. The mean depolarizations induced by the same concentrations of orexin B were 3.3 ± 2.0 mV ($n = 3$) and 7.6 ± 1.1 mV ($n = 12$), respectively. The difference between the depolarizations induced by the same concentrations of orexin A and orexin B was not statistically significant. Orexin A-induced depolarizations were accompanied by an apparent increase in membrane resistance, varying from 10 to 85%, in eight out of 12 neurones (Figs 3*B* and 6*A*); a significant change was not detected in the remaining four neurones. With respect to orexin B-induced depolarizations, an apparent increase in membrane resistance ranging from 20 to 56% was noted in six out of eight neurones.

In a total of 32 neurones to which orexin A and orexin B (100 nM) were applied in a random order, 10 responded to both peptides, one was sensitive to orexin A but not to orexin B, and the remaining neurones did not respond to either peptide.

Effects of orexin on identified PPNs

Intraperitoneal injection of the retrograde tracer Fluoro-gold is an established procedure with which to label autonomic preganglionic neurones in the rat (Leong & Ling, 1990; Merchenthaler, 1991). Identification of PPNs in the DMNV was performed on 33 neurones from 21 rats that had been injected with Fluoro-gold. Twenty-six out of 33 (79 %) DMNV neurones intracellularly labelled with lucifer yellow were also Fluoro-gold positive, and presumed to be PPNs; an example is shown in Fig. 2. The PPNs had a mean resting potential, action potential and input resistance of -54 ± 2 mV ($n = 13$), 68 ± 2 mV ($n = 26$) and 916 ± 106 MΩ ($n = 13$), respectively. Ten of the 33 DMNV neurones were orexin responsive. Nine of the 10 orexin-responsive neurones were double labelled with lucifer yellow and Fluoro-gold (Fig. 2). Of the 10 orexin-responsive neurones, five responded to both orexin A and orexin B, three were tested with orexin B only and the remaining two responded to orexin A only. The characteristics of orexin-induced depolarizations in PPNs were similar to those noted in unidentified DMNV neurones.

Direct excitation by orexin

TTX (0.5 μM), which eliminates the action potentials evoked by a depolarizing current pulse, was added to Krebs solution to block any indirect effects due to the action of orexin on neighbouring neurones. Of the 12 orexin A-responsive DMNV neurones, 10 exhibited a clear depolarization, ranging from 3 to 9 mV, which persisted in TTX-Krebs solution; these included four identified PPNs. In the two neurones where orexin A (and not

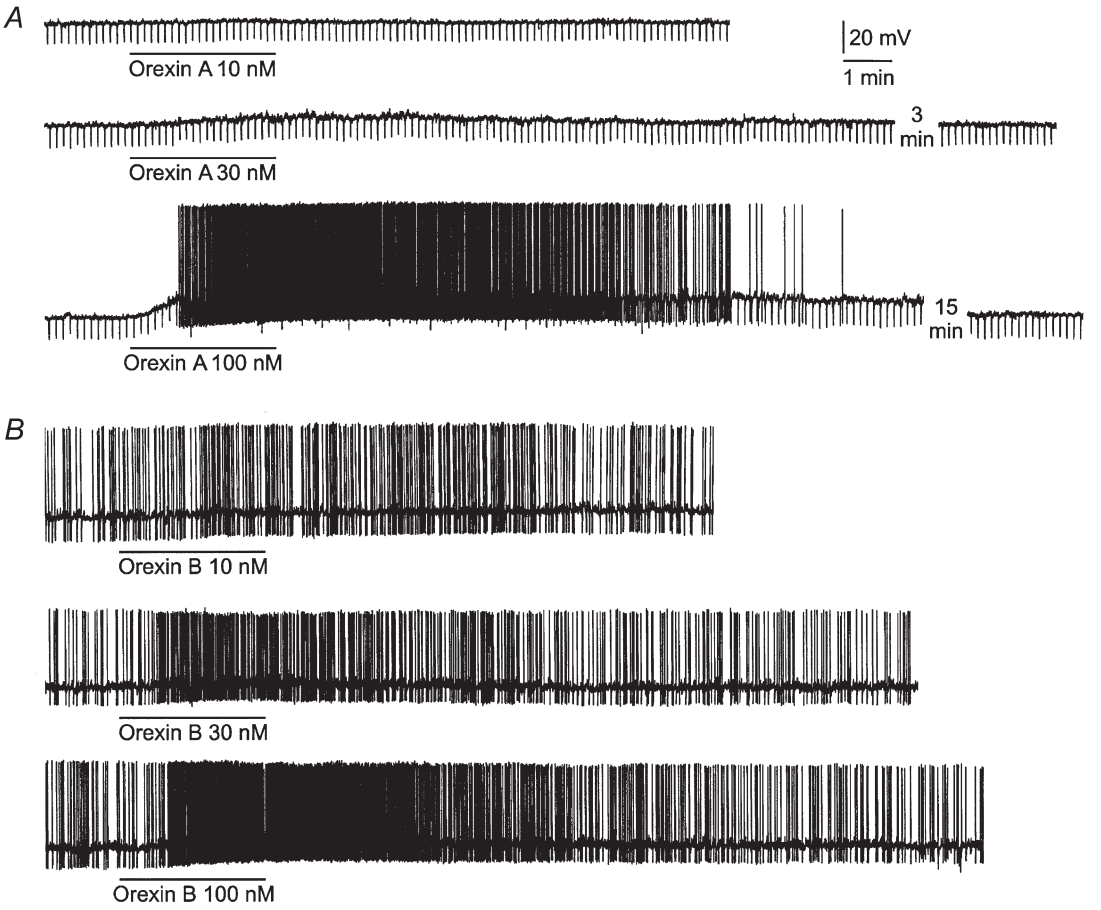

Figure 1. Concentration-dependent orexin-induced depolarizations and discharges from rat DMNV neurones

A, perfusion of orexin A caused a membrane depolarization, the amplitude of which was related to the concentration of peptide applied. Downward deflections are hyperpolarizing electrotonic potentials induced by constant-current pulses (not shown) and were used to monitor the membrane resistance. *B*, orexin B produced a concentration-dependent depolarization and intensified spontaneous discharge. In both neurones, orexin A or orexin B at 10 nM had no apparent effect. At 30 nM, the peptides caused a small depolarization or increased discharge. At 100 nM, the peptides produced a large depolarization and intense discharge lasting for many minutes. The resting membrane potential of the neurones in *A* and *B* was −63 and −51 mV, respectively. The action potentials are truncated due to the limited frequency response of the pen recorder.

orexin B) increased the spontaneous firing frequency, TTX blocked the spontaneous discharges and revealed no underlying depolarization.

Orexin B (100 nM) induced a membrane depolarization and intense discharge in four identified PPNs. In these neurones, TTX eliminated spontaneous discharges and revealed a membrane depolarization varying from 2 to 9 mV.

Ionic basis of orexin-induced depolarizations

An ionic substitution strategy was employed to assess the contribution of Na^+, K^+, or Ca^{2+} ions to orexin A-induced depolarizations (Fig. 3). It was noted during our initial experiments that the responses to a second application of the peptide were smaller in the majority of the neurones tested. To account for this decline in response to a second application of orexin A in normal Krebs solution, the normalized orexin A responses obtained in test solutions were compared with the normalized second responses obtained in normal Krebs solution, which reached $76 \pm 6\%$ of the first responses ($n = 9$; control column in Fig. 3*C*). Under these conditions, the mean orexin A-induced depolarization was reduced to $28 \pm 11\%$ of the mean first response in low-Na^+ (26 mM) solution ($n = 4$, $P < 0.05$), which is significantly different from the mean second orexin A response in normal Krebs solution. In a high-K^+ (7 mM) Krebs solution, the normalized orexin A-induced depolarization was reduced to $60 \pm 10\%$ ($n = 3$), which is statistically insignificant compared to the second mean orexin A response obtained in normal Krebs solution. Representative experiments are shown in Fig. 3*A*. Changing the perfusing solution from Krebs to a low-Na^+ or high-K^+ solution generally caused a shift of less than 5 mV in the resting membrane potential in either direction. In all cases, the membrane potential was restored to the resting level prior to the second application of orexin. The Ca^{2+} channel blocker Cd^{2+} (100 μM) was used to evaluate the role of Ca^{2+} in orexin-induced depolarizations. Experimental protocols were similar to those outlined above. The mean depolarization in Cd^{2+}

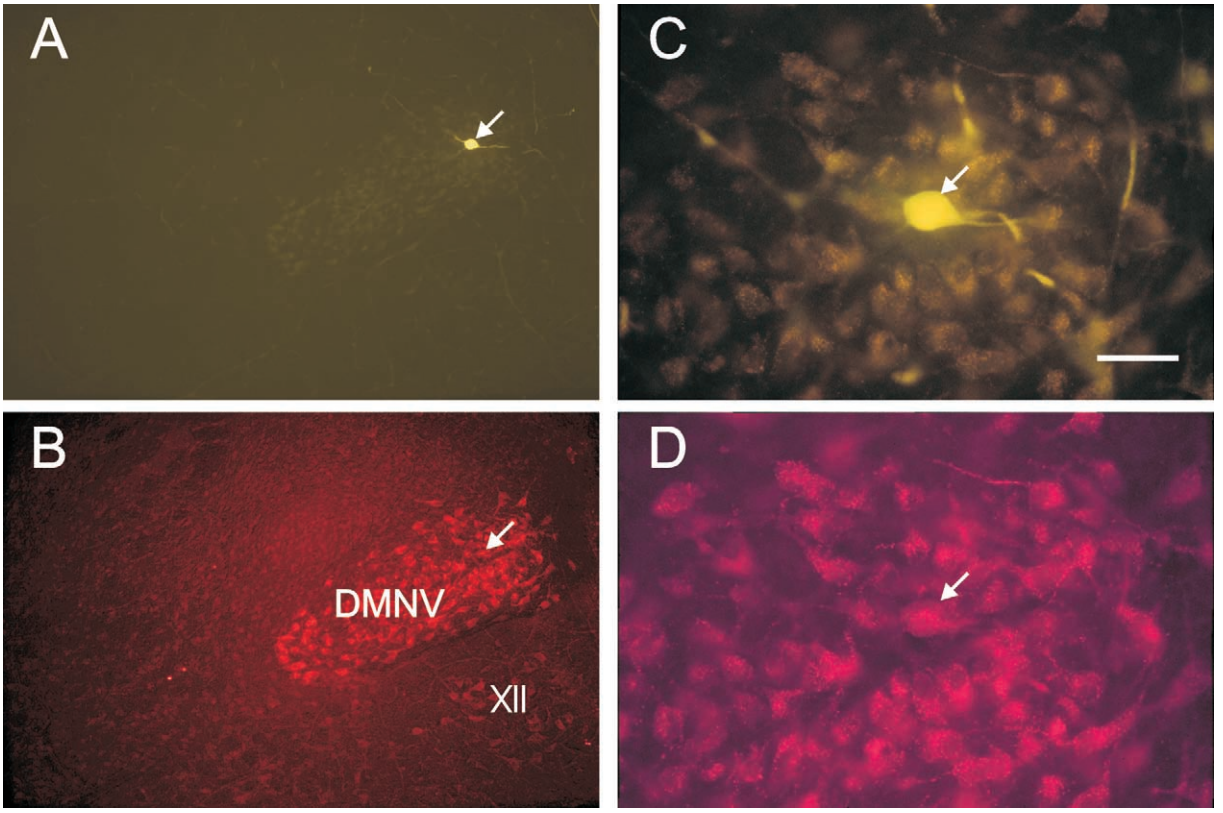

Figure 2. Photomicrographs of a brainstem section through the DMNV double-labelled with lucifer yellow and Fluoro-gold antisera

The rat from which this section was taken received an I.P. injection of Fluoro-gold solution (10 μg) 3 days before recordings were made. *A*, low-magnification micrograph of an orexin-responsive neurone intracellularly labelled with lucifer yellow. *B*, Fluoro-gold-filled DMNV neurones of the same area in the brainstem slice shown in *A*. *C*, higher-magnification micrograph of the lucifer yellow-filled neurone shown in *A*. *D*, higher-magnification micrograph showing the area containing Fluoro-gold-labelled DMNV neurones, one of which is also labelled with lucifer yellow, as shown in *C*. The arrow points to the same neurone in *A*–*D*. Abbreviations: XII, hypoglossal nucleus; DMNV, dorsal motor nucleus of the vagus. Scale bar: 400 μm for *A* and *B* and 50 μm for *C* and *D*.

solution was not significantly different from the second mean orexin A response in normal Krebs solution (Fig. 3*B*). The mean normalized percentage of depolarizations induced by second applications of orexin in normal Krebs solution, and in low-Na^+, high-K^+ solution or Cd^{2+} solution, relative to the normalized responses induced by first applications of orexin, are shown in Fig. 3*C*.

I–V relationships

In this series of experiments, DMNV neurones were voltage clamped to a holding potential of −60 mV. Orexin A and B (100 nM) caused an inward current of 15–120 pA in different neurones tested. The steady-state *I–V* relationship of orexin-induced currents was investigated for orexin A and orexin B in 11 and seven neurones, respectively.

The slope conductance of steady-state *I–V* curves measured in the potential range close to the resting level (from −60 to −70 mV) was decreased in eight out of the 11 neurones tested during orexin A-induced currents (2.6 ± 0.6 *vs.* 2.0 ± 0.7 nS; $P < 0.01$; Fig. 4*A*), and was not changed in the remaining three neurones (Fig. 4*B*). A representative steady-state *I–V* relationship of orexin A-induced currents characterized by a decreased conductance is shown in the right-hand panel of Fig. 4*A*. The orexin A-induced current was decreased with hyperpolarization, but did not reverse polarity in the entire voltage range examined in all eight neurones, including the one shown in Fig. 4*A*.

In the case of orexin B, comparable observations were obtained. The slope conductance was reduced in five of

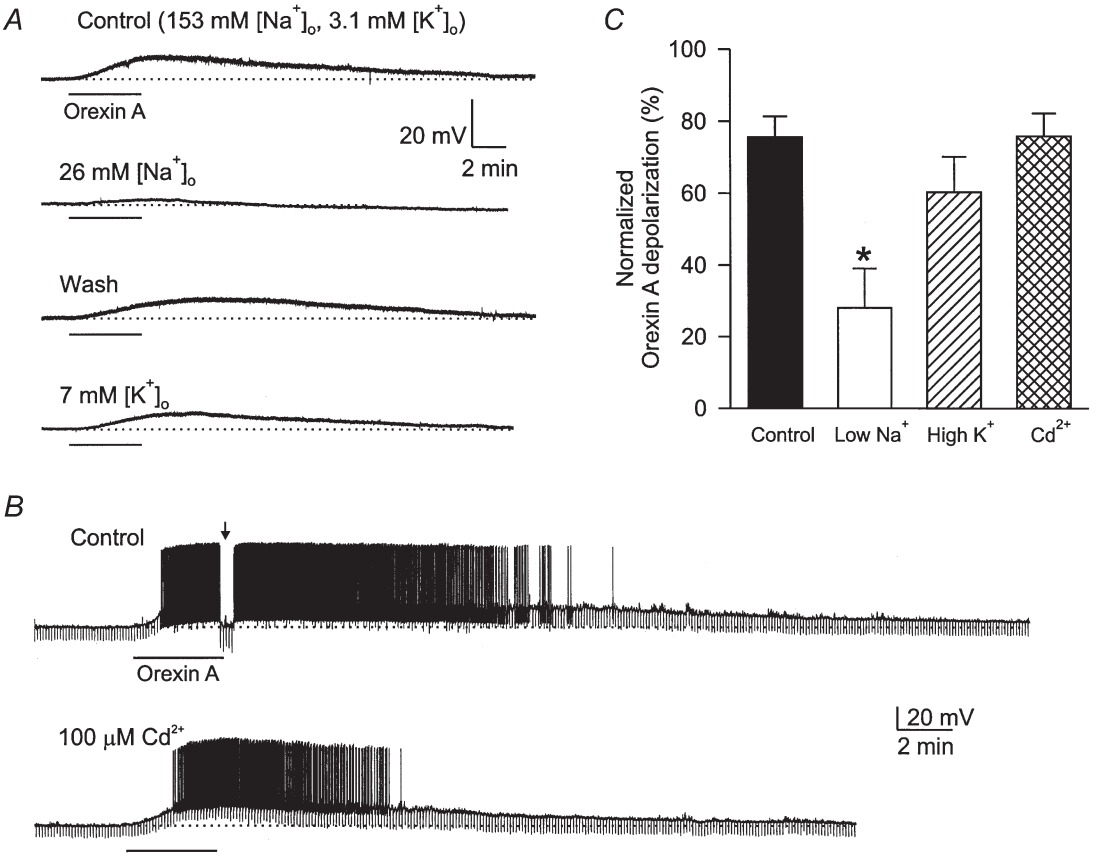

Figure 3. Ionic basis of orexin A-induced depolarizations in DMNV neurones

A, orexin A (100 nM) caused a membrane depolarization in normal Krebs solution containing 153 mM Na^+ and 3.1 mM K^+, which was significantly reduced in a low (26 mM) $[Na^+]_o$ solution. In a high (7 mM) $[K^+]_o$ medium, the orexin A-induced depolarization was also reduced. The resting potential of this neurone was −63 mV; TTX (0.5 μM) was present throughout the experiments. *B*, orexin A (100 nM) induced a membrane depolarization accompanied by intense discharge in normal Krebs solution, and caused a depolarization of similar amplitude in the presence of Cd^{2+} (100 μM). Note that the spike after-hyperpolarization was largely reduced by Cd^{2+}. The arrow indicates that the membrane potential was restored to the control level to measure the input resistance. Dotted lines indicate the original membrane potential at −69 mV. *C*, mean normalized per cent responses of DMNV neurones in various test solutions: low $[Na^+]_o$ ($n = 4$), high $[K^+]_o$ ($n = 3$), Cd^{2+} (100 μM; $n = 4$); the control column represents normalized responses to a second application of orexin A in normal Krebs solution ($n = 9$). *$P < 0.05$ compared to Control.

the seven neurones tested (4.0 ± 1.1 *vs.* 2.8 ± 0.7 nS; $P < 0.05$) and was not changed in the remaining two neurones.

To evaluate the dependency on extracellular Na^+ and K^+ ions, steady-state *I–V* relationships of the orexin-induced currents characterized by a decrease of conductance were measured in a low-Na^+ (26 mM) Krebs solution or in a low-Na^+, high-K^+ (7 mM) Krebs solution in five neurones (three for orexin A and two for orexin B). A representative experiment is shown in Fig. 5. In a low-Na^+ medium, the amplitude of the orexin-induced currents was reduced and the steady-state *I–V* curve reversed polarity at -103 ± 5 mV ($n = 5$). The amplitude of the orexin-induced currents was further decreased and the reversal potential shifted to a more positive level of -88 ± 2 mV ($n = 4$) in a low-Na^+, high-K^+ Krebs solution.

Involvement of GTP-binding proteins

The hydrolysis-resistant guanine nucleotide GDP-β-S was employed to evaluate the possible involvement of GTP-binding proteins in orexin-induced depolarizations. GDP-β-S (1 mM) was added to the patch pipette solution and entered the patched neurone during the course of whole-cell recording.

Either orexin A or orexin B was applied within 10 min after the establishment of the whole-cell configuration, and 40 min after the membrane potential had recovered from the first application of orexin. Responses to the first application of orexin were considered to be control responses and those to the second application were responses after GDP-β-S. For the reason stated above, orexin A and orexin B responses after intracellular perfusion with GDP-β-S were compared statistically with the second responses obtained in normal Krebs solution. The second mean orexin A and orexin B response was $76 \pm 6\%$ ($n = 9$) and $83 \pm 10\%$ ($n = 4$), respectively, of the first mean response obtained in normal Krebs solution. The normalized response to the second application of orexin after intracellular perfusion with GDP-β-S was significantly smaller (orexin A: $18 \pm 11\%$, $n = 5$; orexin B: $35 \pm 15\%$, $n = 4$) as compared to the second response obtained in normal Krebs solution (Fig. 6). The mean resting potential, action potential and input resistance of neurones recorded with the GDP-β-S-containing solution

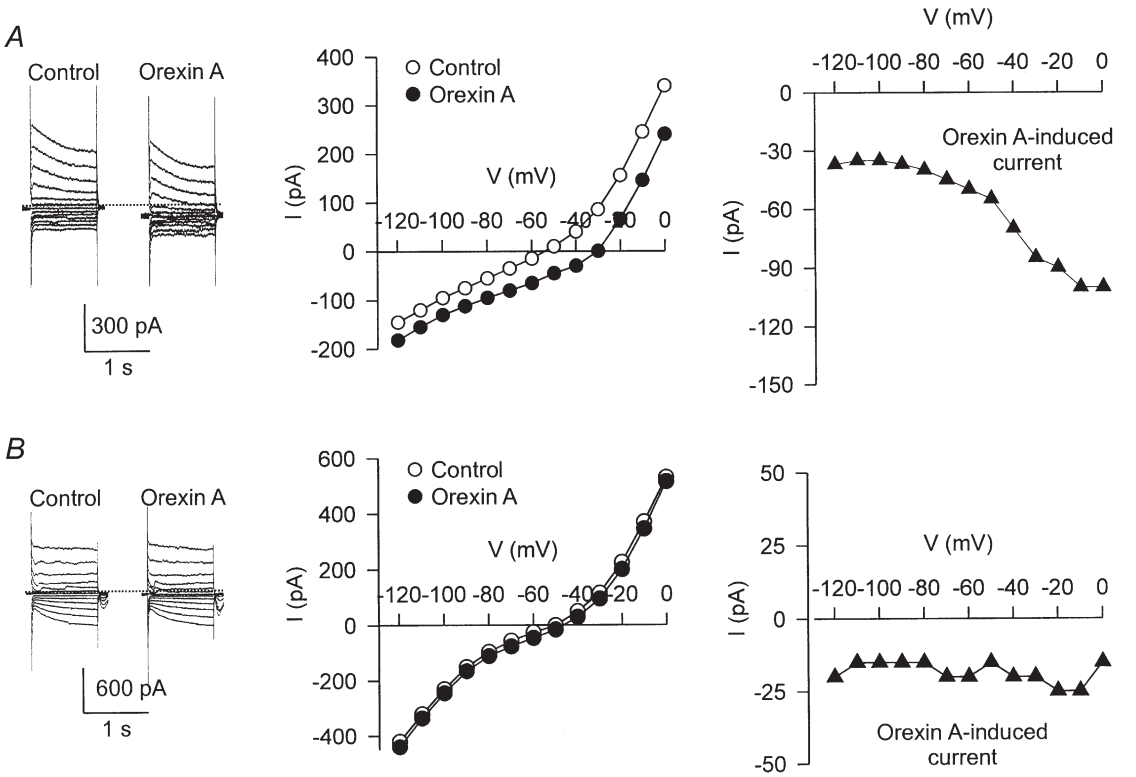

Figure 4. *I–V* relationships of orexin A-induced currents in two DMNV neurones

In *A* and *B*, the panels on the left show the current traces in response to a series of voltage step commands (from −120 to 0 mV) before and during the application of orexin A (100 nM). Small inhibitory postsynaptic currents were noted in the traces shown in *B*. The middle panels show the steady-state *I–V* curves obtained before (open circles) and during (filled circles) the application of orexin A. The difference between these two *I–V* curves represents the *I–V* relationships of orexin-induced currents shown in the panels on the right (filled triangles). The experiments were performed in the presence of TTX (0.5 μM). The dotted lines in the left panels represent the zero holding current.

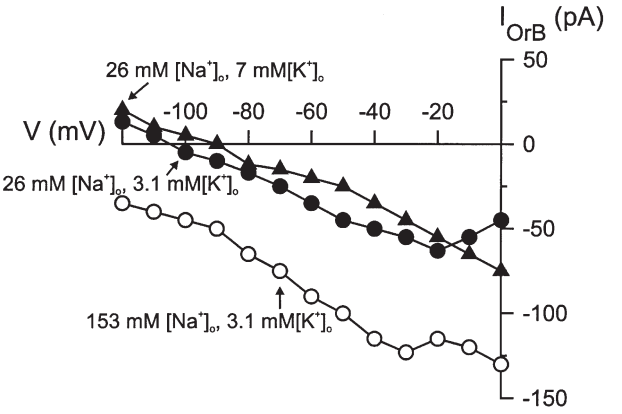

Figure 5. Steady-state *I–V* relationships of orexin B-induced currents in solutions of different ionic concentrations from a single DMNV neurone

Open circles denote responses obtained in normal Krebs solution, filled circles denote responses obtained in a low-Na^+, normal-K^+ Krebs solution, and filled triangles denote those obtained in a low-Na^+, high-K^+ Krebs solution. I_{OrB}, orexin B-induced current.

was -52 ± 2 mV ($n = 21$), 65 ± 2 mV ($n = 28$) and 567 ± 55 MΩ ($n = 21$), respectively, at the onset of recordings. In the majority (~70%) of neurones recorded with the GDP-β-S-containing solution, the membrane potential gradually depolarized and the membrane resistance was either slightly increased or not changed. The mean change in membrane potential and resistance was 6 ± 1 mV ($n = 28$) and 7 ± 3% ($n = 20$) over a period of 40 min. In those neurones where there was a change of membrane potential, it was returned to control levels by current injection prior to the second application of orexin.

DISCUSSION

The present study demonstrates that the hypothalamic peptides orexin A and orexin B are excitatory to DMNV neurones including Fluoro-gold-labelled PPNs, as evidenced by a membrane depolarization and/or increased neuronal discharge. The depolarizations persisted in the presence of both TTX and Cd^{2+}, indicating that the peptides probably acted on the neurones from which the recordings were made. In our study, 79% (26/33) of the recorded DMNV neurones were Fluoro-gold positive,

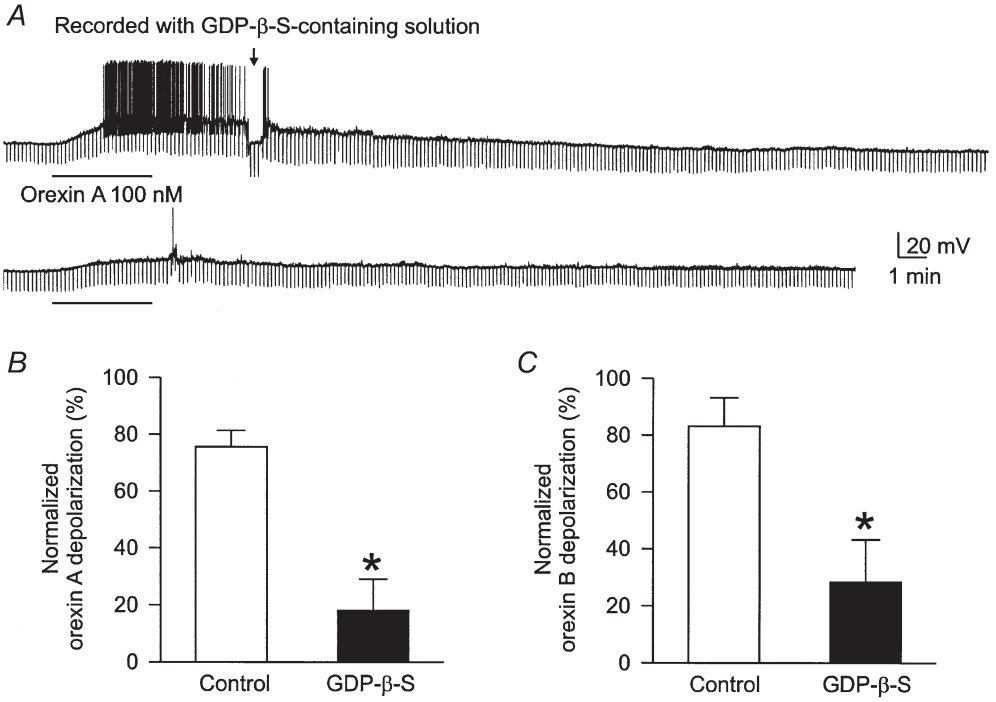

Figure 6. Attenuation of orexin responses in DMNV neurones by intracellular perfusion of GDP-β-S

Neurones were recorded with a glass pipette containing GDP-β-S (1 mM) in the patch solution. *A*, orexin A applied within 10 min after the establishment of whole-cell recording caused a membrane depolarization accompanied by discharge and increased input resistance (arrow). Orexin A, applied again 40 min later, produced a smaller response. The resting membrane potential of this neurone was −59 mV. *B* and *C*, the mean normalized second responses to orexin A and orexin B, respectively, in standard Krebs solution (open columns) and 40 min after intracellular perfusion of GDP-β-S (filled columns); * $P < 0.05$.

indicating that they were indeed PPNs. The remaining Fluoro-gold-negative neurones were probably local circuit interneurones or centrally projecting neurones, as suggested by Loewy & Spyer (1990).

It has been reported that orexins or hypocretins have an excitatory effect on central neurones. Van den Pol *et al.* (1998) showed that hypocretin raises cytoplasmic [Ca^{2+}] and increases the release of GABA or glutamate from cultured medial and lateral hypothalamic and arcuate nucleus neurones by acting on axon terminals. The activation of orexin receptors expressed in Chinese hamster ovary (CHO) cells was shown to cause a phospholipase C-mediated release of Ca^{2+} from intracellular stores, with subsequent Ca^{2+} influx (Smart *et al.* 1999). Our results and those obtained from rat locus coeruleus neurones (Hagan *et al.* 1999; Ivanov & Aston-Jones, 2000) show that the principal effect of orexins is a membrane depolarization. Orexin appears to depolarize locus coeruleus neurones by decreasing the K^+ conductance (Ivanov & Aston-Jones, 2000).

In the case of DMNV neurones, our results suggest that more than one conductance change may be involved. First, orexin-induced depolarizations were significantly reduced in a low-Na^+ Krebs solution, indicating a substantial contribution of Na^+ ions. However, the orexin-induced depolarizations or inward currents were often accompanied by a decrease in membrane conductance, implying that ions other than Na^+ may be involved. A decrease in K^+ conductance seems to be the likely explanation for the decreased membrane conductance associated with responses to orexin. In most cases, the steady-state *I–V* relationship of the orexin-induced inward currents exhibited a decrease in conductance resembling that mediated by a decrease in K^+ conductance, except that a reversal of the orexin-induced currents was not detected in the potential range of −120 to 0 mV. The non-reversal aspect could be explained by a concurrent increase of cation conductance that shifts the *I–V* curve in a negative potential direction. By reducing the concentration of Na^+ ions, the influence of a cation conductance increase on the steady-state *I–V* curve of orexin-induced currents was largely removed. Under this condition, the *I–V* curve was shifted in a more positive direction and a reversal was observed. Thus, the residual orexin-induced current observed in low-Na^+ Krebs solution, which exhibited a negative slope and a reversal potential close to −105 mV, may represent the closure of a K^+ conductance. The calculated K^+ equilibrium potential (E_K) of DMNV neurones is −94 mV at 20 °C under our experimental conditions. The more negative reversal potential obtained experimentally as compared to the predicted E_K may be explained by the residual Na^+ ions in the solution. Moreover, the reversal potential of the orexin-induced current that remained in the low-Na^+ Krebs solution displayed Nernstian behaviour in conditions of high $[K^+]_o$. Collectively, our results suggest that a combined cation conductance increase and K^+ conductance decrease underlies the orexin-induced inward current. The varying degree of contribution from these two mechanisms may explain the differences in the steady-state *I–V* relationship shown in Fig. 4*A* and *B*. A similar mechanism appears to be responsible for the depolarizations induced by a number of peptides and biogenic amines, including neurotensin, in the rat ventral tegmental neurones (Jiang *et al.* 1994) and 5-HT in the rat ventrolateral medulla neurones (Hwang & Dun, 1999).

What might be the ionic basis of the suspected cation conductance? Since orexin-induced depolarizations were not significantly changed by Cd^{2+}, Ca^{2+} ions may not be the major contributor to the depolarizations. The inward current induced by muscarine or neurotensin, which appears to be mediated by a non-selective cation conductance, is also not affected by Ca^{2+}-free solutions or Cd^{2+} (Shen & North, 1992; Jiang *et al.* 1994). A contribution of both K^+ and Na^+ ions may help to explain the relatively insignificant change in orexin-induced depolarizations in high-K^+ Krebs solution. This is because an increase in $[K^+]_i$ could enhance the response mediated by the cation conductance, but would simultaneously reduce the response mediated by the K^+ conductance due to an opposite effect of the high-K^+ Krebs solution on the driving force of these two conductances.

Orexin receptors have been found to be G-protein coupled and show sequence homology (20–30 % identity) with several other peptide receptors including neuropeptide Y, thyrotropin releasing hormone, cholecystokinin A and neurokinin 2 (Sakurai *et al.* 1998). In our study, the inclusion of GDP-β-S, which binds to G-proteins and inhibits the binding of GTP (thereby blocking the GTP-dependent activation of G-proteins), in the patch pipette solution markedly attenuated the responses to orexin in DMNV neurones. Thus, our results are consistent with the idea that the orexin receptor is G-protein coupled.

DMNV neurones are the major source of vagal afferents to the subdiaphragmatic visceral organs, such as the gastrointestinal tract, liver, gallbladder and pancreas (Loewy & Spyer, 1990). In addition, some of the DMNV neurones project to the thoracic viscera, such as the heart and lungs (Kalia, 1981; Stuesse, 1982). A recent study showed that in the rat, intracisternal administration of orexin A but not orexin B stimulates gastric acid secretion, and the response is abolished by vagotomy or administration of atropine, indicating that it is mediated through the central vagal system (Takahashi *et al.* 1999). A stimulatory action of orexin is further corroborated by the finding that intracerebroventricular injection of the peptide induced c-fos expression in DMNV neurones (Date *et al.* 1998). Our observation that orexin depolarizes DMNV neurones including PPNs confirms an excitatory action on these neurones, which may underlie the gastric

acid secretion and c-fos induction by orexin (Date *et al.* 1998; Takahashi *et al.* 1999). Our results, however, appear to differ from those of Takahashi *et al.* (1999) in that orexin B was found to be ineffective in stimulating gastric acid secretion. It has been well documented that PPNs innervating the stomach are predominantly located in the DMNV and that these neurones play a crucial role in the regulation of gastric acid secretion (Laughton & Powley, 1987; Taché, 1987; Okumura & Namiki, 1990; Debas & Carvajal, 1994). An explanation for the apparent discrepancy between our findings and those of Takahashi *et al.* (1999) has yet to be established.

The lateral hypothalamus, which contains the orexin-immunoreactive neurones (de Lecea *et al.* 1998; Sakurai *et al.* 1998; Chen *et al.* 1999), has been identified as one of the key brain sites involved in the control of gastric acid secretion (Taché, 1987). A moderately dense network of orexin A-like immunoreactive fibres has been noted in the DMNV (Date *et al.* 1998; Peyron *et al.* 1998), and these fibres originate from orexin A-containing neurones in the lateral hypothalamus (Harrison *et al.* 1999). These findings suggest that the DMNV is a relay structure for orexin fibres arising from the lateral hypothalamus and projecting to the peripheral organs. The excitatory effect of orexin on the PPNs of the DMNV raises the possibility that in the rat, the peptide released from the lateral hypothalamic neurones modulates the activity of PPNs, which in turn may coordinate gastric secretion (Takahashi *et al.* 1999).

Bernardis, L. L. & Bellinger, L. L. (1993). The lateral hypothalamic area revisited: neuroanatomy, body weight regulation, neuroendocrinology and metabolism. *Neuroscience and Biobehavior Reviews* **17**, 141–193.

Bernardis, L. L. & Bellinger, L. L. (1996). The lateral hypothalamic area revisited: ingestive behavior. *Neuroscience and Biobehavior Reviews* **20**,189–287.

Chen, C. T., Dun, S. L., Kwok, E. H., Dun, N. J. & Chang, J.-K. (1999). Orexin A-like immunoreactivity in the rat brain. *Neuroscience Letters* **260**, 161–164.

Date, Y., Ueta, Y., Yamashita, H., Yamaguchi, H., Matsukura, S., Kangawa, K., Sakurai, T., Yanagisawa, M. & Nakazato, M. (1998). Orexins, orexigenic hypothalamic peptides, interact with autonomic, neuroendocrine and neuroregulatory systems. *Proceedings of the National Academy of Sciences of the USA* **96**, 748–753.

Debas, H. T. & Carvajal, S. H. (1994). Vagal regulation of acid secretion and gastrin release. *Yale Journal of Biology and Medicine* **67**, 145–151.

de Lecea, L., Kilduff, T. S., Peyron, C., Gao, X., Foye, P. E., Danielson, P. E., Fukuhara, C., Battenberg, E. L., Gautvik, V. T., Bartlett, F. S. Ii, Frankel, W. N., van den Pol, A. N., Bloom, F. E., Gautvik, K. M. & Sutcliffe, J. G. (1998). The hypocretins: hypothalamus-specific peptides with neuroexcitatory activity. *Proceedings of the National Academy of Sciences of the USA* **95**, 322–327.

Hagan, J. J., Leslie, R. A., Patel, S., Evans, M. L., Wattam, T. A., Holmes, S., Benham, C. D., Taylor, S. G., Routledge, C., Hemmati, P., Munton, R. P., Ashmeade, T. E., Shah, A. S., Hatcher, J. P., Hatcher, P. D., Jones, D. N. C., Smith, M. I., Piper, D. C., Hunter, A. J., Porter, R. A. & Upton, N. (1999). Orexin A activates locus coeruleus cell firing and increases arousal in the rat. *Proceedings of the National Academy of Sciences of the USA* **96**, 10911–10916.

Harrison, T. A., Chen, C.-T., Dun, N. J. & Chang, J.-K. (1999). Hypothalamic orexin A-immunoreactive neurones project to the rat dorsal medulla. *Neuroscience Letters* **273**, 17–20.

Hwang, L. L. & Dun, N. J. (1998). 5-Hydroxytryptamine responses in immature rat rostral ventrolateral medulla neurones *in vitro*. *Journal of Neurophysiology* **80**, 1033–1041.

Hwang, L. L & Dun, N. J. (1999). 5-HT modulates multiple conductances in immature rat rostral ventrolateral medulla neurones *in vitro*. *Journal of Physiology* **517**, 217–228.

Ivanov, A. & Aston-Jones, G. (2000). Hypocretin/orexin depolarizes and decreases potassium conductance in locus coeruleus neurons. *NeuroReport* **11**, 1755–1758.

Jiang, Z.-G., Pessia, M. & North, R. A. (1994). Neurotensin excitation of rat ventral tegmental neurones. *Journal of Physiology* **474**, 119–129.

Kalia, M. P. (1981). Anatomical organization of central respiratory neurones. *Annual Review of Physiology* **43**, 105–120.

Laughton, W. B. & Powley, T. L. (1987). Localization of efferent function in the dorsal motor nucleus of the vagus. *American Journal of Physiology* **252**, R13–25.

Leong, S.-K. & Ling, E.-A. (1990). Labelling neurones with fluorescent dyes administered via intravenous, subcutaneous or intraperitoneal route. *Journal of Neuroscience Methods* **32**, 15–23.

Loewy, A. D. & Spyer, K. M. (1990). Vagal preganglionic neurones. In *Central Regulation of Autonomic Functions*, ed. Loewy, A. D. & Spyer, K. M., pp. 68–87. Oxford University Press, New York.

Merchenthaler, I. (1991). Neurones with access to the circulation in the central nervous system of the rat: a retrograde tracing study with Fluoro-gold. *Neuroscience* **44**, 655–662.

Okumura, T. & Namiki, M. (1990). Vagal motor neurones innervating the stomach are site-specifically organized in the dorsal motor nucleus of the vagus nerve in rats. *Journal of the Autonomic Nervous System* **29**, 157–162.

Peyron, C., Tighe, D. K., van den Pol, A. N., de Lecea, L., Heller, H. C., Sutcliffe, J. G. & Kilduff, T. S. (1998). Neurones containing hypocretin (orexin) project to multiple neuronal systems. *Journal of Neuroscience* **18**, 9996–10015.

Sakurai, T., Amemiya, A., Ishii, M., Matsuzaki, I., Chemelli, R. M., Tanaka, H., Williams, S. C., Richardson, J. A., Kozlowski, G. P., Wilson, S., Arch, J. R., Buckingham, R. E., Haynes, A. C., Carr, S. A., Annan, R. S., McNulty, D. E., Liu, W. S., Terrett, J. A., Elshourbagy, N. A., Bergsma, D. J. & Yanagisawa, M. (1998). Orexins and orexin receptors: a family of hypothalamic neuropeptides and G protein-coupled receptors that regulate feeding behavior. *Cell* **92**, 573–585.

Shen, K.-Z. & North, R. A. (1992). Muscarine increases cation conductance and decreases potassium conductance in rat locus coeruleus. *Journal of Physiology* **455**, 471–485.

Smart, D., Jerman, J. C., Brough, S. J., Rushton, S. L., Murdock, P. R., Jewitt, F., Elshourbagy, N. A., Ellis, C. E., Middlemiss, D. N. & Brown, F. (1999). Characterization of recombinant human orexin receptor pharmacology in a Chinese hamster ovary cell-line using FLIPR. *British Journal of Pharmacology* **128**, 1–3.

Stuesse, S. L. (1982). Origins of cardiac vagal preganglionic fibres: a retrograde transport study. *Brain Research* **236**, 15–25.

Taché, Y. (1987). Central regulation of gastric acid secretion. In *Physiology of the Gastrointestinal Tract*, 2nd edn, ed. Johnson, J. R., Christensen, J., Jackson, M., Jacobson, E. D. & Walsh, J. H., pp. 911–930. Raven Press, New York.

Takahashi, N., Okumura, T., Yamada, H. & Kohgo, Y. (1999). Stimulation of gastric acid secretion by centrally administered orexin-A in conscious rats. *Biochemical and Biophysical Research Communications* **254**, 623–627.

Van den Pol, A. N., Gao, X. B., Obrietan, K., Kilduff, T. S. & Belousov, A. B. (1998). Presynaptic and postsynaptic actions and modulation of neuroendocrine neurones by a new hypothalamic peptide, hypocretin/orexin. *Journal of Neuroscience* **18**, 7962–7971.

Yamamoto, Y., Ueta, Y., Date, Y., Nakazato, M., Hara, Y., Serino, R., Nomura, M., Shibuya, I., Matsukura, S. & Yamashita, H. (1999). Down regulation of the prepro-orexin gene expression in genetically obese mice. *Molecular Brain Research* **65**, 14–22.

Acknowledgements

This study was supported by NIH grants NS18710 and HL51314 from the Department of Heath and Human Services.

Corresponding author

N. J. Dun: Department of Pharmacology, James H. Quillen College of Medicine, East Tennessee State University, PO Box 70577, Johnson City, TN 37614, USA.

Email: dunnae@etsu.edu

Authors' present addresses

L.-L. Hwang: Department of Physiology, Taipei Medical University, Taipei, Taiwan.

C.-T. Chen: Division of Biotechnology and Pharmaceutical Research, National Health Research Institutes, Taipei, Taiwan.